

"DEAD" LAYERS IN FERROMAGNETIC TRANSITION METALS*

L. Liebermann and J. Clinton
University of California, La Jolla, California 92037

and

D. M. Edwards and J. Mathon†
Imperial College, London, S. W. 7, England
(Received 1 June 1970)

Magnetically "dead" layers, previously observed in iron films at room temperature, are observed in nickel. From the temperature dependence of this effect it is deduced that two dead layers persist at $T=0$, independent of the film thickness. Existing theories of magnetic thin films are unable to account for these observations. The existence of dead layers at $T=0$ is attributed to a transfer of electrons from the s band to the d band in the neighborhood of a surface. This effect is incorporated in Stoner's theory of ferromagnetism and the results on the temperature dependence of the number of dead layers are in good agreement with experiment.

A new effect in ferromagnetism was recently observed in iron films.¹ It was found that at room temperature every iron film apparently has two magnetically "dead" layers; no theory was proposed for this effect. In this Letter we report new work on nickel films in which the dead-layer effect is even more striking. The variation of the number of dead layers with temperature is investigated and it is shown that these effects can be understood on the basis of an itinerant-electron theory of ferromagnetism.

Production of nearly continuous, nonstressed, and unoxidized thin nickel films must be achieved in order to observe these effects properly. Formation by electroplating from an aqueous solution of nickel salts was found to be superior (compared with vacuum evaporation) for film production. Film uniformity was checked by the voltaic method described previously.¹ Film thickness was obtained from the electrolytic current and the time. The ferromagnetic flux was observed by the change in induced voltage between two coils, one of which was powered by the line frequency (60 Hz) at levels to produce saturation in

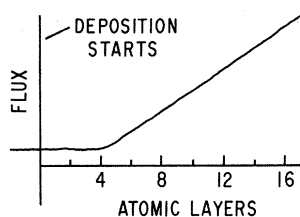


FIG. 1. Recording of the saturation flux as the thickness of a nickel film is continuously increased by electrolytic deposition. Four dead layers (or their equivalent) remain dead as the film thickness continues to grow.

the plane of the film. The induced voltage was electronically integrated to give a signal proportional to the saturation flux.

The observation method is illustrated by the recording shown in Fig. 1 which gives the observed magnetic flux in a nickel film as the thickness is continuously increased by electroplating onto a nonmagnetic substrate. Note particularly

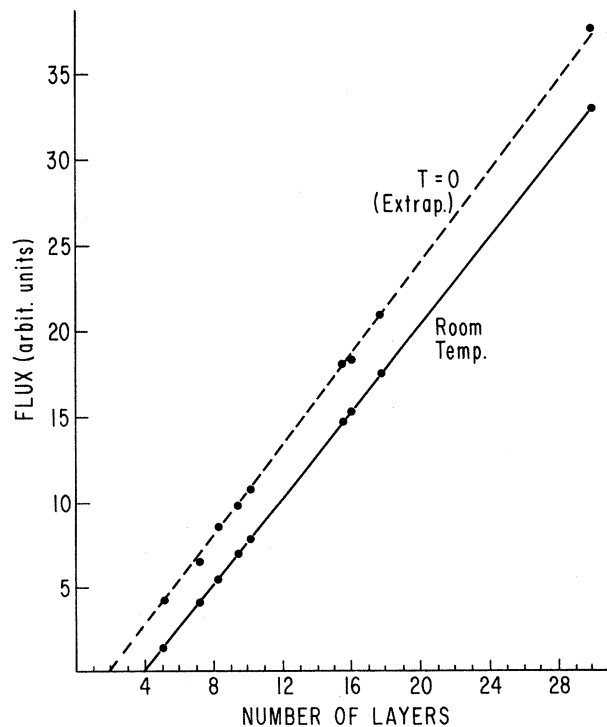


FIG. 2. Relative flux versus thickness for a number of discrete nickel samples. The zero-flux intercept denotes four dead layers at room temperature and two dead layers at $T=0$.

that the flux contribution of four atomic layers remains absent regardless of the film thickness. This recording is precisely reproducible for a large number of independent trials at room temperature. Similar records have been obtained for iron¹ and for cobalt,² using the same experimental techniques.

The possibility that magnetically "dead" layers are the result of diffusion of the substrate into the ferromagnetic film appears to have been eliminated by the use of different substrates, i.e. copper and gold, without discernible effect; additionally, the flux is unchanged by deposition of copper on the free film surface.

Figure 2 gives data for nickel which permit extrapolation of the number of dead layers to absolute zero. Each point on the straight lines represents a discrete nickel film sample of designated thickness. Note that the zero-flux intercept yields four dead layers at room temperature, consistent with the data of Fig. 1, and two dead layers at $T=0$. The data points on the line designated $T=0$ are from the same discrete samples as observed at room temperature but are obtained by extrapolation from temperature-variation measurements. As an example, Fig. 3 gives the thermal variation of magnetization in two discrete samples of 7- and 17-atomic-layer thickness; each point represents observations at the designated temperature.

The existence of dead layers implies that the magnetization, averaged over the sample, is of

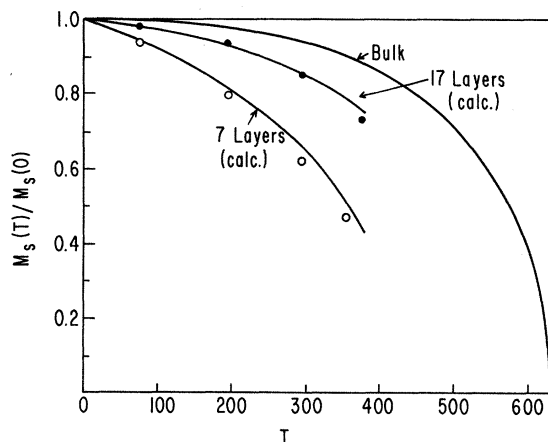


FIG. 3. Thermal variation of magnetization for two discrete samples: 7 and 17 atomic layers. Each point represents observation at the designated temperature. The smooth curves are theoretical; predicted deviation of film behavior from the bulk arises solely from the theoretical variation of the number of dead layers with temperature.

the form

$$M = M_B - \alpha/D, \quad (1)$$

where M_B is the bulk magnetization, D is the number of atomic layers in the film, and α is proportional to the number of dead layers. Although the standard external-field spin-wave theory of films³ yields a magnetization of this form, for the Heisenberg model $\alpha \rightarrow 0$ as $T \rightarrow 0$ which is contrary to the present observation of two dead layers at $T=0$. Furthermore, the magnitude of α at room temperature is much too small to fit our experiments. The existence of dead layers in Ni at $T=0$, and the temperature variation, is accounted for in an itinerant-electron theory presented below. Clearly spin-wave effects are also present in an itinerant-electron model but here we adopt a molecular-field approach which is a direct extension of bulk Stoner theory. The loss of magnetic moment compared with the bulk occurs only in the neighborhood of the surfaces and, since interaction with the substrate appears to be unimportant, it may be assumed that this loss occurs equally at both surfaces. We use the symbol d to represent the number of dead layers per surface, so that $d=1$ at $T=0$ for nickel.

The magnetic carriers in nickel are holes in the d band and in the bulk all their spins are aligned at $T=0$. The observed loss of moment near the surface could be due either to a local reduction in the number of d holes, or to occupied hole states of opposite spin bound at the surface by the exchange potential. Detailed calculation shows that the exchange potential is not sufficiently strong to produce such a surface state. A loss of d holes near the surface is to be expected on the basis of the tight-binding approximation for the d band and is best discussed in terms of electrons rather than holes. The top of the d band in bulk Ni is at the three distinct points X in the Brillouin zone. States near the top of the band, corresponding to \vec{k} near $(0, 0, 2\pi/a)$ in the bulk, have approximate wave functions of the form

$$\psi \propto \sum_{\vec{R}} \vec{r} \exp[i(k_x \xi + k_y \eta)] \varphi(\vec{r} - \vec{R}) \text{sinc } k_z \zeta \quad (2)$$

for a $(0, 0, 1)$ surface. The summation is over atomic sites $\vec{R} = (\xi, \eta, \zeta)$ in the semi-infinite metal and the plane $\zeta=0$ is a distance $\frac{1}{2}a$ outside the surface. The wave functions (2) rise only slowly from zero at $\zeta=0$, i.e., like $\text{sinc } k_z' \zeta$ where $k_z' = k_z - 2\pi/a$ is small. The situation for states corresponding to the other two X points is more complicated. The existence of an ordinary non-

magnetic surface state near the bottom of the d band⁴ would result in further reduced weight at the surface for states near the top of the d band. Thus, the effect of introducing 0.6 holes/atom into the top of the d band, as in nickel, is to remove fewer electrons near the surface than in the bulk. A similar boundary-condition effect gives a reduced s -electron density near the surface, as calculated for a jellium model,⁵ and s - d Coulomb interaction will enhance both effects. We therefore predict an s - d transfer near the surface. To account for the observation of one dead layer per surface at $T=0$ a transfer of 0.6 electrons per surface atom is required.

Low⁶ has shown that in the presence of carriers of both spins, as in nickel at finite temperatures, a local charge-density disturbance leads to a magnetic disturbance of longer range. The range of the magnetic disturbance depends on the bulk properties of the ferromagnetic metal and not on the precise nature of the local charge disturbance. It is therefore possible to discuss the magnetic effects of the reduced d -hole density near the surface by considering a simple model of a uniform gas of positively charged d holes perturbed by the introduction of a positively charged plane at $z=0$. A slightly more realistic model would be that of a two-component gas, corresponding to d holes and s electrons, but since the s electrons screen much less efficiently, owing to their low density of states, we adopt the simpler model. Following Low, the Fourier components $\delta\rho_{\uparrow q}$ and $\delta\rho_{\downarrow q}$ of the resultant changes in hole density are given approximately by the two equations

$$\delta\rho_{\sigma q} = \chi_{\sigma q} \{ V_q + (4\pi e^2/q^2)(\delta\rho_{\uparrow q} + \delta\rho_{\downarrow q}) - I\delta\rho_{\sigma q} \}, \quad (3)$$

where σ corresponds to \uparrow or \downarrow spin, V_q is the Fourier component of the potential due to the charged plane, and I is an exchange parameter related to the parameter θ' of Stoner theory. The density-density response function $\chi_{\sigma q}$ is taken as that for a noninteracting gas of σ -spin holes with density $\rho_{\sigma}(T)$ given by Stoner theory. In our calculations we assume a parabolic band with mass m^* and choose m^* and I so that, appropriately for Ni,⁷ the spins are just completely aligned at $T=0$ and the Curie temperature $T_C = 630^\circ\text{K}$. It follows from (3) that

$$\delta M_q(T) = \delta\rho_{\uparrow q} - \delta\rho_{\downarrow q} = \Gamma_q(T) \delta M_0(0), \quad (4)$$

where, for small q , $\Gamma_q(T)$ is of the form

$$\Gamma_q(T) = \frac{\chi_{\uparrow 0} - \chi_{\downarrow 0}}{(\chi_{\uparrow 0} + \chi_{\downarrow 0} + 2I\chi_{\uparrow 0}\chi_{\downarrow 0})(1 + q^2/k^2)}. \quad (5)$$

The corresponding spatial dependence of the loss of magnetic moment due to the perturbation is $\delta M(z, T) = \delta M_0(T) \kappa e^{-\kappa z}$. The range κ^{-1} is essentially a normal screening length at $T=0$ but increases with temperature and behaves as $(T_C - T)^{-1/2}$ near T_C . This behavior should be contrasted to that of the density change $\delta\rho(z, T) + \delta\rho_0(z, T)$, the total density loss being independent of temperature and the range parameter being always of the order of a screening length.

The number of dead layers d , calculated consistently within the present Stoner-type theory, is proportional to $|\delta M_0(T)|/M(T)$, where $M(T)$ is the calculated bulk magnetization. Thus,

$$d(T) = [\Gamma_0(T)M(0)/M(T)]d_0, \quad (6)$$

where d_0 is the number of dead layers at $T=0$. For a film D layers thick the reduced spontaneous magnetization is given by

$$\frac{M_s(T)}{M_s(0)} = \frac{D - 2d(T)M_B(T)}{D - 2d_0M_B(0)}. \quad (7)$$

Here $M_B(T)$ is taken to be the observed bulk Ni magnetization, so that deviations of $M_s(T)/M_s(0)$ from bulk behavior are due to a true dead-layer effect and not to deviations of the bulk Stoner magnetization $M(T)$ from the observed $M_B(T)$. The only adjustable parameter in the theory is d_0 , which represents the extent of the s - d electron transfer at the surface and is taken to fit the experimental value $d_0 = 1$ at $T=0$. Numerical results compared with experiment are shown in Fig. 3 for films of 7 and 17 layers. As T_C is approached the linear response calculation of $\delta M_0(T)$ breaks down and interference effects between the surfaces must also be considered.

The authors wish to acknowledge helpful discussions with E. P. Wohlfarth and K. D. Leaver.

*Work supported in part by the U. S. Office of Naval Research.

†Present address: The City University, London.

¹L. N. Liebermann, D. R. Fredkin, and H. B. Shore, *Phys. Rev. Lett.* **22**, 539 (1969).

²L. Liebermann, unpublished results. Cobalt, like iron, shows two layers remaining nonmagnetic.

³I. S. Jacobs and C. P. Bean, in *Magnetism*, edited by G. T. Rado and H. Suhl (Academic, New York 1963), Vol III.

⁴F. Forstmann, to be published.⁵N. D. Lang, Solid State Commun. **7**, 1047 (1969).⁶G. G. Low, Proc. Phys. Soc., London **92**, 938

(1967).

⁷E. P. Wohlfarth, Proc. Roy. Soc., London, Ser. A **195**, 434 (1949).COUPLING OF ELASTIC WAVES TO THE "NONACTIVATED" SPIN-FLOP MODE IN MnF₂†

R. L. Melcher*

Laboratory of Atomic and Solid State Physics, Cornell University, Ithaca, New York 14850

(Received 16 June 1970)

The coupling of the nonactivated spin-flop mode in MnF₂ to two elastic modes via the linear magnetoelastic interaction is shown to lead to discontinuities at the spin-flop transition in the elastic constants c_{11} and $c' = \frac{1}{2}(c_{11} - c_{12})$. The directions of easy magnetization in the basal plane are determined to be the equivalent [110] axes.

In this paper we demonstrate that basal-plane anisotropy and/or hyperfine coupling to the Mn⁵⁵ nuclear spin system lead to an energy gap at zero wave vector ($q=0$) in the energy spectrum of the so-called "nonactivated" spin-flop mode (NASFM) in the nominally uniaxial antiferromagnet MnF₂. The linear magnetoelastic interaction couples this mode to the elastic modes $c' = \frac{1}{2}(c_{11} - c_{12})$ and c_{11} ,¹ producing large, almost discontinuous decreases in these two elastic constants at the spin-flop transition. This represents the first definite experimental detection of the NASFM. The symmetry of these two elastic modes is sufficient to conclude that the directions of easy magnetization in the basal plane of MnF₂ are the equivalent [110] axes. It is suggested that the coupling of the NASFM to these elastic modes is responsible for the "absorption edges" reported by Šapira and Zak at the spin-flop transition of MnF₂.²

In the usual approximation of uniaxial symmetry the spin wave frequencies at $q=0$ are found to be³

$$\omega_{\pm} = \gamma(H_c \pm H_0), \quad H_0 < H_c; \quad (1)$$

$$\omega_{s-f} = \gamma(H_0^2 - H_c^2)^{1/2} \quad (2a)$$

and

$$\omega_{NA} = 0, \quad H_0 < H_c, \quad (2b)$$

where γ is the gyromagnetic ratio, $H_c \equiv (2H_E H_A)^{1/2}$ is the spin-flop field ($H_c \approx 93$ kG in MnF₂ at 4.2°K), H_E and H_A are, respectively, the exchange and uniaxial anisotropy fields, and H_0 is the dc magnetic field applied along the "easy" axis (the easy direction in MnF₂ is the [001] axis).⁴

The macroscopic fourfold symmetry of MnF₂ about the [001] axis makes possible an additional contribution to the magnetic anisotropy energy which we take to have the following single-ion

form:

$$E_A(\text{basal plane}) = -\frac{1}{2} \frac{K'}{M_0^4} (M_{1x}^2 M_{1y}^2 + M_{2x}^2 M_{2y}^2), \quad (3)$$

where $H_A' = |K'|/M_0$ is the in-plane anisotropy field, M_{ij} is the j th component ($j=x, y, z$) of the i th sublattice magnetization ($i=1, 2$), and $M_0^2 = \sum_j M_{1j}^2 = \sum_j M_{2j}^2$. In addition, the strong hyperfine interaction between the Mn⁵⁵ nuclear spin and the electronic spin of the Mn⁺⁺ ion leads to an effective nuclear anisotropy field $H_N \approx 9/T$ G (T = nuclear spin temperature) which acts along the equilibrium direction of the electronic sublattice.^{5,6} In the approximation $H_A \gg H_A', H_N$, the modes ω_{\pm} and ω_{s-f} [Eqs. (1) and (2a)] are unchanged. However, an energy gap appears in the spectrum for ω_{NA} at $q=0$ given by

$$\omega_{NA} = \gamma[2H_E(H_A' + H_N)]^{1/2}, \quad (4)$$

where terms of order $(H_0/H_E)^2$ have been neglected. This result is independent of the sign of K' .

The coupling of elastic modes to the NASFM via the linear magnetoelastic interaction depends crucially on the sign of K' . Using a general form of the interaction reflecting the tetragonal symmetry of MnF₂, two types of coupling occur:

(1) As found previously,⁷ the mode c_{44} couples to ω_{-} if $H_0 < H_c$ and to ω_{s-f} if $H_0 > H_c$. The coupling constant in both cases is designated b_5 . (2) When $H_0 > H_c$, either c' and c_{11} or c_L and c_{66} couple to the NASFM (depending on the sign of K'). Since the NASFM does not exist for $H_0 < H_c$ and since ω_{NA} is independent of H_0 for $H_0 > H_c$, this coupling produces discontinuous shifts $\Delta c_{ij} \equiv c_{ij}(H_0 < H_c) - c_{ij}(H_0 > H_c)$ at the spin-flop phase boundary ($H_0 \approx H_c$). The calculated Δc_{ij} for the assumption K'